

# Complex Frequency

Federico Milano, *IEEE Fellow*

**Abstract**—The paper introduces the concept of *complex frequency*. The imaginary part of the complex frequency is the variation with respect of a synchronous reference of the local bus frequency as commonly defined in power system studies. The real part is defined based on the variation of the voltage magnitude. The latter term is crucial for the correct interpretation and analysis of the variation of the frequency at each bus of the network. The paper also develops a set of differential equations that describe the link between complex powers and complex frequencies at network buses in transient conditions. No simplifications are assumed except for constant elements of the network admittance matrix. A variety of analytical and numerical examples show the applications and potentials of the proposed concept.

**Index Terms**—Power system dynamics, converter-interfaced generation, frequency control, low-inertia systems.

## I. INTRODUCTION

A well-known and accepted definition of the frequency of a signal  $x(t) = X_m(t) \cos(\vartheta(t))$  is given in the IEEE Std. IEC/IEEE 60255-118-1 [1], as follows:

$$f(t) = \frac{1}{2\pi} \dot{\vartheta}(t) = \frac{1}{2\pi} \dot{\theta}(t) + f_o, \quad (1)$$

where  $\theta$  is the phase difference, in radians, between the angular position  $\vartheta$ , also in radians, of the signal  $x(t)$  and the phase due to the reference nominal frequency  $f_o$ , expressed in Hz. If the magnitude  $X_m$  of the signal is constant, this definition is adequate. However, if  $X_m$  changes with time, the definition of the frequency in (1) does not provide a meaningful way to separate the effects of the variations of  $\vartheta$  and  $X_m$ . Thus, the definition of frequency in the most general conditions is a highly controversial concept that has been discussed at length in the literature (see the interesting discussion in [2] and the references therein).

This paper provides a novel interpretation of “frequency” as complex quantity, i.e., composed of a real and an imaginary part. This *complex frequency* takes into account the time dependency of both  $\vartheta$  and  $X_m$ . The focus is on the theory, modeling, simulation and some application aspects of the proposed definition. The proposed complex frequency allows a neat and compact representation as well as a consistent interpretation of frequency variations in ac power systems. The complex frequency is also capable of explaining the interactions among active and reactive power injections at buses and flows in network branches. It is important to note that the proposed approach does not attempt to substitute

the modelling approaches that go beyond the classical phasor representation or that focus on analysis of non-sinusoidal signals (see, for example, [3] for a state-of-the-art survey on this topic and the several references therein). On the contrary, the proposed concept of “complex frequency” is compatible with the approaches that have been proposed in the literature as it allows interpreting angle and magnitude variations as complementary components of the same phenomenon, provided that one accepts to extend the domain of frequency to the complex numbers.

This paper focuses on electro-mechanical transients in high-voltage transmission systems. Thus, the starting point is similar to that of [4]–[7], that is, the transient conditions during which the magnitude and the phase angle of bus voltage phasors change according to the inertial response of synchronous machines and the frequency control of synchronous and non-synchronous devices. On the other hand, harmonics, unbalanced conditions and electro-magnetic transients are not taken into consideration.

The resulting formulation is *exact*, in the measure that power system models based on the dqo transform for voltage and angle stability analysis are exact; *general*, as it provides a framework to study the dynamic effect of any device on the local frequency variations at network buses; and *systematic*, because it provides with the tools to determine analytically the impact of each device on bus frequencies.

The remainder of the paper is organized as follows. Section II provides the background for the proposed theoretical framework. Section III provides the formal definition of *complex frequency* and its link with complex power injections, voltage and current dynamic phasors and network topology. The special cases of constant power and constant current injections as well as constant impedances are discussed in Section III-C. Section III-D discusses a variety of relevant approximated expressions that link the complex frequency to bus power injections. Section IV illustrates some applications of the analytical expressions derived in Section III to simulation, state estimation and control. Finally, Section V draws conclusions and outlines future work.

## II. BACKGROUND

The starting point is the set of equations that describe the complex power injections, in per unit, at the  $n$  network buses of the system, say  $\bar{s} \in \mathbb{C}^n$ , as follows:

$$\bar{s}(t) = \mathbf{p}(t) + \mathbf{jq}(t) = \bar{\mathbf{v}}(t) \circ \bar{\mathbf{i}}^*(t), \quad (2)$$

where  $\mathbf{p} \in \mathbb{R}^{n \times 1}$  and  $\mathbf{q} \in \mathbb{R}^{n \times 1}$  are the active and reactive power injections at network buses, respectively;  $\bar{\mathbf{v}} \in \mathbb{C}^{n \times 1}$  and  $\bar{\mathbf{i}} \in \mathbb{C}^{n \times 1}$  are the dynamic voltage and injection current phasors at network buses; \* indicates the conjugate of a

F. Milano is with the School of Electrical & Electronic Engineering, University College Dublin, Belfield, Ireland. E-mail: federico.milano@ucd.ie

This work was supported by Science Foundation Ireland, by funding F. Milano under project AMPSAS, Grant No. SFI/15/IA/3074; and by the European Commission by funding F. Milano under project EdgeFLEX, Grant No. 883710.

complex quantity; and  $\circ$  is the Hadamard product, i.e. the element-by-element product of two vectors.<sup>1</sup> It is important to note that (2) is valid in transient conditions [8]. On the other hand, in steady-state, balanced conditions, (2) expresses the well-known power flow equations.

In this context, *dynamic phasor* means the dq-axis components of the well-known dqo transform of the voltages and currents. For example, for the voltage, one has:

$$\bar{\mathbf{v}}(t) = \mathbf{v}_d(t) + j\mathbf{v}_q(t). \quad (3)$$

where the components  $v_{d,k}$  and  $v_{q,k}$  of the  $k$ -th element of the vector  $\bar{\mathbf{v}}$  are calculated as follows:

$$\begin{bmatrix} v_{d,k}(t) \\ v_{q,k}(t) \\ v_{o,k}(t) \end{bmatrix} = \mathbf{P}(t) \begin{bmatrix} v_{a,k}(t) \\ v_{b,k}(t) \\ v_{c,k}(t) \end{bmatrix}, \quad (4)$$

where

$$\mathbf{P}(t) = \sqrt{\frac{2}{3}} \begin{bmatrix} \cos(\alpha(t)) & \cos(\alpha'(t)) & \cos(\alpha''(t)) \\ \sin(\alpha(t)) & \sin(\alpha'(t)) & \sin(\alpha''(t)) \\ \frac{1}{\sqrt{2}} & \frac{1}{\sqrt{2}} & \frac{1}{\sqrt{2}} \end{bmatrix}, \quad (5)$$

and  $\alpha$  is the angle between the phase a and the q-axis, with  $\dot{\alpha} = \omega_o$ , and  $\alpha' = \alpha - \frac{2\pi}{3}$  and  $\alpha'' = \alpha + \frac{2\pi}{3}$ . The same transformation (4) is applied to the abc currents. Since no assumption is made on the abc quantities, the d- and q-axis components of the dynamic phasors  $\bar{\mathbf{v}}$  and  $\bar{\mathbf{i}}$  and, hence, (2) are valid in transient conditions, i.e., for non-sinusoidal abc quantities.

The  $v_{o,k}$  is the o-axis or *zero* component and is null for balanced systems. If the system is not balanced and the o-axis components are not null, then the vector  $\mathbf{p}$  in (2) does not represent the total active power injections at network buses as it does not include the term  $\mathbf{v}_o \circ \mathbf{i}_o$ . The hypothesis of balanced system is not necessary for the developments presented below. However, since the focus is on high-voltage transmission systems, in the remainder of this paper, balanced, positive sequence operating conditions are assumed.

For the purposes of the developments given below, it is convenient to rewrite (3) in polar form:

$$\bar{\mathbf{v}}(t) = \mathbf{v}(t) \circ \angle\boldsymbol{\theta}(t), \quad (6)$$

where  $\mathbf{v} = |\bar{\mathbf{v}}|$ ,  $\angle\boldsymbol{\theta} = \cos(\boldsymbol{\theta}) + j\sin(\boldsymbol{\theta})$  and

$$\boldsymbol{\theta}(t) = \boldsymbol{\vartheta}(t) - \theta_o(t), \quad (7)$$

namely,  $\boldsymbol{\theta}$  is the vector of bus voltage phase angles referred to the rotating dq-axis reference frame,  $\boldsymbol{\vartheta}$  are the bus voltage phase angles referred to a constant reference and  $\theta_o = \int_t \omega_o dt$  is the angle of the rotating dq-axis reference frame and  $\omega_o$  is the angular frequency in rad/s of the dq-axis reference frame.

From (1), the time derivative of  $\boldsymbol{\theta}$  gives:

$$\boldsymbol{\omega}(t) = \dot{\boldsymbol{\theta}}(t) = \dot{\boldsymbol{\vartheta}}(t) - \omega_o(t), \quad (8)$$

where  $\boldsymbol{\omega}$  is the vector of frequency deviations with respect to the reference frequency at the network buses. In [1], it is assumed that  $\omega_o = 2\pi f_o$  is constant and equal to the nominal

angular frequency of the grid, e.g.,  $\omega_o = 2\pi 60$  rad/s in North American transmission grids. Note, however, that  $\omega_o$  being constant is not a requirement of the derivations given in the remainder of this paper. As a matter of fact, in the examples presented in Section IV,  $\omega_o$  is set to be equal to the frequency of the Center of Inertia (CoI).

We now introduce the only approximation of the whole derivations given in this section, i.e., we assume that the link between current injections and voltages is given by

$$\bar{\mathbf{i}}(t) \approx \bar{\mathbf{Y}} \bar{\mathbf{v}}(t), \quad (9)$$

where  $\bar{\mathbf{Y}} = \mathbf{G} + j\mathbf{B} \in \mathbb{C}^{n \times n}$  is the conventional admittance matrix of the network. It is important not to confuse (9) with the conventional relationship between current and voltage phasors (in which case (9) is an exact equality).  $\bar{\mathbf{i}}$  and  $\bar{\mathbf{v}}$  are “dynamic” complex quantities and, hence, (9) represents an approximation of the dynamics of the grid. In turn, to obtain (9), it is assumed that, for network inductances and capacitances the relationships between voltages and currents can be approximated with:

$$\begin{aligned} \bar{v} &= L\dot{\bar{i}} \approx j\omega_o L\bar{i} = jX\bar{i}, \\ \bar{i} &= C\dot{\bar{v}} \approx j\omega_o C\bar{v} = jB\bar{v}, \end{aligned} \quad (10)$$

where  $L$ ,  $C$ ,  $X$ ,  $B$  are the inductance, capacitance, reactance and susceptance, respectively. The approximation above assumes that electro-magnetic transients in the elements of the transmission lines and transformers are *fast* and can be assumed to be in Quasi-Steady-State (QSS). This is the conventional approximation utilized in RMS models for angle and voltage stability analysis [9]. The focus of this paper is, in fact, on the time scales of electro-mechanical and primary frequency and voltage control transients, which are a few orders of magnitude slower than electro-magnetic dynamics.

Merging (2) and (9) becomes:

$$\bar{\mathbf{s}}(t) = \bar{\mathbf{v}}(t) \circ [\bar{\mathbf{Y}} \bar{\mathbf{v}}(t)]^*. \quad (11)$$

These equations resemble the well-known power flow equations except for the fact that the voltages and, hence, the power injections at buses are time-varying quantities.

#### A. Time Derivative of Algebraic Equations

An important aspect of the developments discussed in the next section is whether (11) can be differentiated with respect to an independent variable and, in particular, with respect to time. With this aim, observe that (9) leads to the well-known QSS model for power system angle and voltage transient stability analysis, as follows [9], [10]:

$$\begin{aligned} \dot{\mathbf{x}} &= \mathbf{f}(\mathbf{x}, \mathbf{y}, \mathbf{z}), \\ \mathbf{0} &= \mathbf{g}(\mathbf{x}, \mathbf{y}, \mathbf{z}), \end{aligned} \quad (12)$$

where  $\mathbf{f} \in \mathbb{R}^{n_x + n_y + n_z} \mapsto \mathbb{R}^{n_x}$  are the differential equations;  $\mathbf{g} \in \mathbb{R}^{n_x + n_y + n_z} \mapsto \mathbb{R}^{n_y}$  are the algebraic equations,  $\mathbf{x} \in \mathcal{X} \subset \mathbb{R}^{n_x}$  are the state variables;  $\mathbf{y} \in \mathcal{Y} \subset \mathbb{R}^{n_y}$  are the algebraic variables; and  $\mathbf{z} \in \mathcal{Z} \subset \mathbb{R}^{n_z}$  are discrete variables that defines events such as line outages and faults. In practice, discrete variables can be modelled as *if-then* rules that modify the structure of  $\mathbf{f}$  and  $\mathbf{g}$ , and, hence, they do not require additional equations.

<sup>1</sup>The Hadamard product of two column vectors  $\mathbf{x}$  and  $\mathbf{z}$  can be also written as  $\mathbf{x} \circ \mathbf{z} = \text{diag}(\mathbf{x}) \mathbf{z}$ , where  $\text{diag}(\mathbf{x})$  is a diagonal matrix whose element  $(i, i)$  is the  $i$ -th element of the vector  $\mathbf{x}$ .

The set of Differential-Algebraic Equations (DAEs) in (12) is continuous except for a finite set of points where the discrete variables  $\mathbf{z}$  change their value. The implicit function theorem indicates that, if the Jacobian matrix  $\partial \mathbf{g} / \partial \mathbf{y}$  is not singular, there exists a function  $\phi$  such that:

$$\mathbf{y} = \phi(\mathbf{x}, \mathbf{z}). \quad (13)$$

Equation (13) is often utilized to reduce the set of DAEs in (12) into a set of Ordinary Differential Equations (ODEs) that depends only on  $\mathbf{x}$  and  $\mathbf{z}$ . In this work, however, (13) is utilized the other way round, i.e., to guarantee that it is possible to define the time derivative of  $\mathbf{y}$  except for the finite number of points where an element of vector  $\mathbf{z}$  changes value. This condition leads to:

$$\begin{aligned} \dot{\mathbf{y}} &= \frac{\partial \phi}{\partial \mathbf{x}} \dot{\mathbf{x}} = \left( \frac{\partial \mathbf{g}}{\partial \mathbf{y}} \right)^{-1} \frac{\partial \mathbf{g}}{\partial \mathbf{x}} \dot{\mathbf{x}} \\ &= \left( \frac{\partial \mathbf{g}}{\partial \mathbf{y}} \right)^{-1} \frac{\partial \mathbf{g}}{\partial \mathbf{x}} \mathbf{f}(\mathbf{x}, \phi(\mathbf{x}, \mathbf{z}), \mathbf{z}). \end{aligned} \quad (14)$$

The condition (14) implies that the set of DAEs in (12) is assumed to be *index 1* [11], which is the form of DAEs that describes most physical systems, including power systems [10].

The voltage magnitudes  $\mathbf{v}$  and phase angles  $\boldsymbol{\theta}$  that appears in (11), and hence also the real and imaginary parts of the complex power  $\bar{\mathbf{s}}$ , are algebraic variables in the conventional formulation of QSS models. Thus, the assumption of index-1 DAEs allows rewriting the current injections at bus and, hence, the complex power  $\bar{\mathbf{s}}$  as functions of state and discrete variables, as well as of the bus voltages  $\bar{\mathbf{v}}$ , namely  $\bar{\mathbf{s}}(\bar{\mathbf{v}}, \mathbf{x}, \mathbf{z})$ , which are smooth, except at the points where the elements of  $\mathbf{z}$  transition from one value to another. Then, the time derivatives of  $\bar{\mathbf{s}}$  can be computed with the chain rule as:

$$\dot{\bar{\mathbf{s}}} = \frac{\partial \bar{\mathbf{s}}}{\partial \bar{\mathbf{v}}} \dot{\bar{\mathbf{v}}} + \frac{\partial \bar{\mathbf{s}}}{\partial \mathbf{x}} \dot{\mathbf{x}}. \quad (15)$$

The next section of this paper elaborates on (15) and deduces an expression that involves the concept of complex frequency.

### III. DERIVATION

For the sake of the derivation, it is convenient to drop the dependency on time and rewrite (11) in an element-wise notation. For a network with  $n$  buses, one has:

$$\begin{aligned} p_h &= v_h \sum_{k=1}^n v_k [G_{hk} \cos \theta_{hk} + B_{hk} \sin \theta_{hk}], \\ q_h &= v_h \sum_{k=1}^n v_k [G_{hk} \sin \theta_{hk} - B_{hk} \cos \theta_{hk}], \end{aligned} \quad (16)$$

where  $G_{hk}$  and  $B_{hk}$  are the real and imaginary parts of the element  $(h, k)$  of the network admittance matrix, i.e.  $\bar{Y}_{hk} = G_{hk} + jB_{hk}$ ;  $v_h$  and  $v_k$  denote the voltage magnitudes at buses  $h$  and  $k$ , respectively; and  $\theta_{hk} = \theta_h - \theta_k$ , where  $\theta_h$  and  $\theta_k$  are the voltage phase angles at buses  $h$  and  $k$ , respectively. Equations (16) and all equations with subindex  $h$  in the remainder of this section are valid for  $h = 1, 2, \dots, n$ .

Equations (16) can be equivalently written as:

$$p_h = \sum_{k=1}^n p_{hk}, \quad \text{and} \quad q_h = \sum_{k=1}^n q_{hk}, \quad (17)$$

where

$$\begin{aligned} p_{hk} &= v_h v_k [G_{hk} \cos \theta_{hk} + B_{hk} \sin \theta_{hk}], \\ q_{hk} &= v_h v_k [G_{hk} \sin \theta_{hk} - B_{hk} \cos \theta_{hk}]. \end{aligned} \quad (18)$$

Differentiating (16) and writing the active power injections as the sum of two components:

$$dp_h = \sum_{k=1}^n \frac{\partial p_h}{\partial \theta_{hk}} d\theta_{hk} + \sum_{k=1}^n \frac{\partial p_h}{\partial v_k} dv_k \equiv dp'_h + dp''_h, \quad (19)$$

In (19),  $dp_h$  is the total variation of power at bus  $h$ ;  $dp'_h$  is the quota of the active power that depends on bus voltage phase angle variations; and  $dp''_h$  is the quota of active power that depends on bus voltage magnitude variations. From (11) and using the same procedure that leads to (19), one can define two components also for the reactive power, as follows:

$$dq_h = \sum_{k=1}^n \frac{\partial q_h}{\partial \theta_{hk}} d\theta_{hk} + \sum_{k=1}^n \frac{\partial q_h}{\partial v_k} dv_k \equiv dq'_h + dq''_h. \quad (20)$$

From (17), it is relevant to observe that:

$$\frac{\partial p_h}{\partial \theta_{hk}} = -q_{hk}, \quad \text{and} \quad \frac{\partial q_h}{\partial \theta_{hk}} = p_{hk}, \quad (21)$$

which leads to rewrite  $dp'_h$  and  $dq'_h$  as:

$$\begin{aligned} dp'_h &= -\sum_{k=1}^n q_{hk} d\theta_{hk}, \\ dq'_h &= \sum_{k=1}^n p_{hk} d\theta_{hk}, \end{aligned} \quad (22)$$

Recalling that  $\theta_{hk} = \theta_h - \theta_k$ , one has:

$$\begin{aligned} dp'_h &= -q_h d\theta_h + \sum_{k=1}^n q_{hk} d\theta_k, \\ dq'_h &= p_h d\theta_h - \sum_{k=1}^n p_{hk} d\theta_k, \end{aligned} \quad (23)$$

where the identities (17) have been used.

In the same vein, from (17), (19) and (20),  $dp''_h$  and  $dq''_h$  can be rewritten as:

$$\begin{aligned} dp''_h &= \frac{p_h}{v_h} dv_h + \sum_{k=1}^n \frac{p_{hk}}{v_k} dv_k, \\ dq''_h &= \frac{q_h}{v_h} dv_h + \sum_{k=1}^n \frac{q_{hk}}{v_k} dv_k. \end{aligned} \quad (24)$$

Let us define the quantity:

$$u_h \equiv \ln(v_h), \quad (25)$$

where  $v_h$  is expressed in per unit and  $u_h$  is dimensionless. The differential of (25) gives:

$$du_h = \frac{dv_h}{v_h}. \quad (26)$$

Then, (24) can be rewritten as:

$$\begin{aligned} dp''_h &= p_h du_h + \sum_{k=1}^n p_{hk} du_k, \\ dq''_h &= q_h du_h + \sum_{k=1}^n q_{hk} du_k. \end{aligned} \quad (27)$$

Equations (23) and (27) can be expressed in terms of complex powers variations:

$$\begin{aligned} d\bar{s}'_h &= dp'_h + j dq'_h = j \bar{s}_h d\theta_h - j \sum_{k=1}^n \bar{s}_{hk} d\theta_k, \\ d\bar{s}''_h &= dp''_h + j dq''_h = \bar{s}_h du_h + \sum_{k=1}^n \bar{s}_{hk} du_k, \end{aligned} \quad (28)$$

and, finally, defining the complex quantity:

$$\bar{\zeta}_h \equiv u_h + j\theta_h, \quad (29)$$

the total complex power variation is given by:

$$\begin{aligned} d\bar{s}_h &= d\bar{s}'_h + d\bar{s}''_h \\ &= dp'_h + dp''_h + j(dq'_h + dq''_h) \\ &= \bar{s}_h d\bar{\zeta}_h + \sum_{k=1}^n \bar{s}_{hk} d\bar{\zeta}_k^* \end{aligned} \quad (30)$$

Equation (30) can be written in a compact matrix form, as follows:

$$d\bar{s} = \bar{s} \circ d\bar{\zeta} + \bar{\mathbf{S}} d\bar{\zeta}^*, \quad (31)$$

where  $\bar{\mathbf{S}} \in \mathbb{C}^{n \times n}$  is a matrix whose  $(h, k)$ -th element is  $\bar{s}_{hk}$ .

The expression (31) has been obtained in general, i.e., assuming a differentiation with respect to a generic independent parameter. If this parameter is the time  $t$ , (31) can be rewritten as a set of differential equations:

$$\dot{\bar{s}} - \bar{s} \circ \bar{\eta} = \bar{\mathbf{S}} \bar{\eta}^* \quad (32)$$

where

$$\bar{\eta} = \dot{\bar{\zeta}} = \dot{\mathbf{u}} + j\dot{\theta}, \quad (33)$$

and recalling the derivative of  $\theta$  given in (8) and defining  $\boldsymbol{\varrho} \equiv \dot{\mathbf{u}}$ , one obtains:

$$\bar{\eta} \equiv \boldsymbol{\varrho} + j\boldsymbol{\omega} \quad (34)$$

We define  $\bar{\eta}$  as the vector of *complex frequencies* of the buses of an AC grid. Note that both real and imaginary part of (34) have, in fact, the dimension of  $s^{-1}$ , as  $\mathbf{u}$  is dimensionless and  $\boldsymbol{\omega}$  is expressed in rad/s. In (34), the imaginary part is the usual angular frequency (relative to the reference  $\omega_o$ ). On the other hand, it is more involved to determine the physical meaning of the real part of (34),  $\boldsymbol{\varrho}$ . From the definition of  $u_h$ , one has  $v_h = \exp(u_h)$ , that is, the magnitude of the voltage is expressed as a function whose derivative is equal to the function itself. This concept is key in the theory of Lie groups and algebra, which defines the space of linear transformations of generalized ‘‘rates of change’’ [12].

Equation (32) is the sought expression of the relationship between frequency variations and power flows in an ac grid. It contains the information on how power injections of the devices connected to the grid impact on the frequency at their point of connection as well as on the rest of the grid. In (32), the elements of  $\bar{s}$  are the inputs or *boundary conditions* at network buses and depend on the devices connected to grid, whereas  $\bar{\mathbf{S}}$  depends only on network quantities.

Another way to write (32) is by splitting  $\dot{\bar{s}}$  into its components  $\dot{\bar{s}}'$  and  $\dot{\bar{s}}''$ . According the definitions of  $\bar{s}'$  and  $\bar{s}''$ ,  $\dot{\bar{s}}'$  does not depend on  $\boldsymbol{\varrho}$ , whereas  $\dot{\bar{s}}''$  does not depend on  $\boldsymbol{\omega}$ , as follows:

$$\begin{aligned} \dot{\bar{s}}' &= j\bar{s} \circ \boldsymbol{\omega} - j\bar{\mathbf{S}} \boldsymbol{\omega}, \\ \dot{\bar{s}}'' &= \bar{s} \circ \boldsymbol{\varrho} + \bar{\mathbf{S}} \boldsymbol{\varrho}. \end{aligned} \quad (35)$$

It is important to note that, in general, the expressions of  $\dot{\bar{s}}'$  and  $\dot{\bar{s}}''$  are not known *a priori*. These components, however, can be determined using (32), (35) and:

$$\dot{\bar{s}} = \dot{\bar{s}}' + \dot{\bar{s}}'' \quad (36)$$

With this regard, Section IV-B explains through an example how to calculate  $\boldsymbol{\omega}$  and  $\boldsymbol{\varrho}$  based on (32). In the following, (32), (35) and (36) are utilized to discuss relevant special cases.

### A. Alternative Expressions

We now derive (32) in an alternative and more compact formulation as a function of the currents. First, observe that:

$$\dot{\bar{v}} = \bar{v} \circ \bar{\eta}. \quad (37)$$

The proof of (37) is given in the Appendix. Then, recalling (2), the time derivative of  $\bar{s}$  with respect to the dq-axis reference frame can be written as:<sup>2</sup>

$$\begin{aligned} \dot{\bar{s}} &= \frac{d}{dt} (\bar{v} \circ \bar{\mathbf{i}}^*) \\ &= \dot{\bar{v}} \circ \bar{\mathbf{i}}^* + \bar{v} \circ \dot{\bar{\mathbf{i}}}^* \\ &= \bar{v} \circ \bar{\eta} \circ \bar{\mathbf{i}}^* + \bar{v} \circ \dot{\bar{\mathbf{i}}}^* \\ &= \bar{s} \circ \bar{\eta} + \bar{v} \circ \dot{\bar{\mathbf{i}}}^*. \end{aligned} \quad (38)$$

Substituting (38) into (32), one obtains:

$$\bar{v} \circ \dot{\bar{\mathbf{i}}}^* = \bar{\mathbf{S}} \bar{\eta}^* \quad (39)$$

Yet another way to write (32) can be obtained by deriving with respect of time (9), or, which is the same, dividing each row  $h$  of  $\bar{\mathbf{S}}$  by the corresponding voltage  $\bar{v}_h$  in (39). This leads to (see also footnote 1):

$$\dot{\bar{\mathbf{i}}} = \bar{\mathbf{Y}} [\bar{v} \circ \bar{\eta}] = \bar{\mathbf{Y}} \text{diag}(\bar{v}) \bar{\eta}, \quad (40)$$

and, defining  $\bar{\mathbf{I}} = \bar{\mathbf{Y}} \text{diag}(\bar{v})$ , one obtains:

$$\dot{\bar{\mathbf{i}}} = \bar{\mathbf{I}} \bar{\eta} \quad (41)$$

As per (32), the right-hand sides of (39) and (41) depend exclusively on network quantities, whereas the left-hand side is device dependent. While equivalent, the relevant feature of (39) and (41) with respect to (32) is that the complex frequency vector only appears once.

### B. Remarks on the Complex Frequency of Current Injections

Equation (41) also indicates that, in transient conditions, the frequency of the current injections at network buses is not the same as the frequency of the voltages at the same buses. Let assume that  $\bar{v}_h = v_h \angle \beta_h$ , then, one has:

$$\dot{\bar{v}}_h = \bar{v}_h \left( \frac{\dot{v}_h}{v_h} + j\dot{\beta}_h \right) = \bar{v}_h \bar{\xi}_h, \quad (42)$$

where  $\bar{\xi}_h$  is the complex frequency of the current injection at bus  $h$  which is determined using the same procedure that leads to (37) and that is described in the Appendix. Note that, in general,  $\bar{\xi}_h \neq \bar{\eta}_h$ . A relevant special case is that of constant power factor devices (either generators or loads), for which

<sup>2</sup>Note that the Hadamard product is commutative. Note also that, in a rotating frame such as the one defined by the dqo transform, the total time derivative of (2) is given by:

$$\dot{\bar{s}} + j\omega_o \bar{s} = \frac{d}{dt} (\bar{v} \circ \bar{\mathbf{i}}^*) + j\omega_o (\bar{v} \circ \bar{\mathbf{i}}^*),$$

where  $j\omega_o$  is due to the angular rotation of dq-axis. However, since (2) has to be always satisfied, the terms that are multiplied by  $j\omega_o$  can be removed for the expression above, thus leading to (32). In this paper, only the time derivative with respect to the rotating dq-axis is considered. This means that the imaginary part of the complex frequency represents the variations with respect to  $\omega_o$ .

$\beta_h = \theta_h + \varphi_{ho}$ , where  $\varphi_{ho}$  is the constant power factor angle. Then:

$$\dot{\beta}_h = \dot{\theta}_h + \dot{\varphi}_{ho} = \omega_h. \quad (43)$$

On the other hand,  $\text{Re}\{\bar{\xi}_h\} = \varrho_h$  only if  $v_h = kv_h$ . Since constant impedances have constant power factor and their current is proportional to the voltage, they satisfy the condition  $\bar{\xi}_h = \bar{\eta}_h \forall t$ . Finally, (41) is also particularly suitable for the calculation of  $\bar{\eta}$  in a software tool as it only requires to express the current injections at each bus  $h$  as a function of  $v_h$  and/or the state variables of the device connected at the bus. Some examples of this procedure are given in Section IV.

### C. Special Cases

Three cases are considered in this section, namely, constant power injection, constant current injection, and constant admittance load. These cases illustrate the utilization of the formulas deduced above, namely (32), (39) and (41).

1) *Constant Power Injection*: We illustrate first an application of (32) for a constant power injection, say  $\bar{s}_h = \bar{s}_{ho}$ . From (36), the boundary condition at the  $h$ -th bus is:

$$\dot{\bar{s}}_h = 0 \quad \Rightarrow \quad \dot{\bar{s}}'_h = -\dot{\bar{s}}''_h, \quad (44)$$

and, from (35):

$$j\bar{s}_{ho}\omega_h - j\sum_{k=1}^n \bar{s}_{hk}\omega_k = -\bar{s}_{ho}\varrho_h - \sum_{k=1}^n \bar{s}_{hk}\varrho_k, \quad (45)$$

and, from (32):

$$-\bar{s}_{ho}\bar{\eta}_h = \sum_{k=1}^n \bar{s}_{hk}\bar{\eta}_k^*. \quad (46)$$

2) *Constant Admittance Load*: This case illustrates an application of (39). For a constant admittance load, the current consumption at the  $h$ -th bus is:

$$\bar{v}_h = -\bar{Y}_{ho}\bar{v}_h, \quad (47)$$

where the negative sign indicates that the current is drawn from bus  $h$ . From (39) and (47) and recalling that  $\dot{v}_h = \bar{v}_h\bar{\eta}_h$  (see the Appendix), one obtains:

$$-\bar{Y}_{ho}^*v_h^2\bar{\eta}_h^* = \sum_{k=1}^n \bar{s}_{hk}\bar{\eta}_k^*. \quad (48)$$

The same result can be obtained also from (32). The power consumption at bus  $h$  can be written as:

$$\bar{s}_h = \bar{v}_h\bar{v}_h^* = -\bar{Y}_{ho}^*v_h^2, \quad (49)$$

which indicates that the power consumption  $\bar{s}_h$  in (49) does not depend on  $\theta_h$ . Hence, from (36),  $\bar{s}_h = \bar{s}''_h$  and  $\bar{s}'_h = 0$ . From the first equation of (35), one has:

$$-\bar{Y}_{ho}^*v_h^2\omega_h = \bar{s}_h\omega_h = \sum_{k=1}^n \bar{s}_{hk}\omega_k. \quad (50)$$

Then, from the time derivative of (49) and the second equation of (35), one has:

$$-2\bar{Y}_{ho}^*v_h\dot{v}_h = -\bar{Y}_{ho}^*v_h^2\varrho_h + \sum_{k=1}^n \bar{s}_{hk}\varrho_k. \quad (51)$$

Observing that, from (26),  $\varrho_h = \dot{v}_h/v_h$ , then:

$$v_h\dot{v}_h = v_h^2\varrho_h, \quad (52)$$

and, hence, (51) can be rewritten as:

$$-\bar{Y}_{ho}^*v_h^2\varrho_h = \bar{s}_h\varrho_h = \sum_{k=1}^n \bar{s}_{hk}\varrho_k, \quad (53)$$

The expressions (50) and (53) have the same structure and can be merged into (48). Moreover, in the summations on the right-hand-sides of (48), the term  $\bar{s}_{hh}$  is given by:

$$\bar{s}_{hh} = \bar{Y}_{hh}^*v_h^2, \quad (54)$$

and, defining  $\bar{Y}_{h,\text{tot}} = \bar{Y}_{ho} + \bar{Y}_{hh}$ , one obtains:

$$-\bar{Y}_{h,\text{tot}}^*v_h^2\bar{\eta}_h^* = \sum_{h \neq k}^n \bar{s}_{hk}\bar{\eta}_k^*, \quad (55)$$

which indicates that the two components of the complex frequency,  $\varrho_h$  and  $\omega_h$  at the bus  $h$  of a constant admittance load are linear combinations of the  $\varrho_k$  and  $\omega_k$  at the neighboring buses. This, in turn and as expected, means that constant admittance loads are *passive* devices and cannot modify the frequency at their point of connection but rather “take” the frequency that is imposed by the rest of the grid. This conclusion generalizes the results of the appendix of [7] that considers the simplified case of an admittance load connected to the rest of the system through a lossless line.

3) *Constant Current Injection*: This last example shows an application of (41). For a constant current injection, we have two cases. If the magnitude and phase angle of the current are constant, then  $\dot{i}_h = 0$  and, from (41), one obtains immediately:

$$0 = \sum_{k=1}^n \bar{v}_{hk}\bar{\eta}_k, \quad (56)$$

where,  $\bar{v}_{hk}$  is the  $(h, k)$  element of  $\bar{\mathbf{I}}$ . Equivalently, from (39), the condition  $\dot{i}_h = 0$  leads to:

$$0 = \sum_{k=1}^n \bar{s}_{hk}\bar{\eta}_k^*. \quad (57)$$

On the other hand, it is unlikely that a device is able to impose the phase angle of its current injection independently from the phase angle of its bus voltage. More likely, a device imposes a constant magnitude and power factor. In this case, the phase angle of the current  $\beta_h$  depends on the phase angle  $\theta_h$  of the voltage at bus  $h$  as discussed in Section III-B. Hence,  $\bar{s}''_h = 0$  and  $\bar{s}_h = \bar{s}'_h$ . This result generalizes the one obtained in [13]. From (41), a current injection with constant magnitude and power factor leads to:

$$\begin{aligned} \dot{i}_h &= j\sum_{k=1}^n \bar{v}_{hk}\omega_k, \\ 0 &= \sum_{k=1}^n \bar{v}_{hk}\varrho_k, \end{aligned} \quad (58)$$

and, since  $\dot{\beta}_h = \omega_h$  (see Section III-B and (43)), the first equation of (58) can be rewritten as:

$$\text{Re}\{\bar{\xi}_h\} = \frac{i_h}{v_h} = -j\left(\omega_h - \sum_{k=1}^n \frac{\bar{v}_{hk}}{v_h}\omega_k\right). \quad (59)$$

### D. Approximated Expressions

The mathematical developments carried out so far have assumed no simplifications except for neglecting the electro-magnetic dynamics of network branches. All formulas that have been deduced are thus accurate in the measure that the effect of electro-magnetic transients are negligible. It is, however, relevant to explore whether the expressions (32), (39) and (41) can be approximated while retaining the information on the relationship between power injections and frequency variations at network buses.

Except during faults, which in any case have to last few tens of milliseconds to prevent generators to loose synchronism, one can assume that  $v_h \approx 1$  pu and that bus voltage phase angle differences are small, hence  $\sin(\theta_h - \theta_k) \approx \theta_h - \theta_k$  and  $\cos(\theta_h - \theta_k) \approx 1$ . These assumptions, which, in turn, are the well-known approximation utilized in the fast decoupled power flow method [14], lead to:

$$\bar{s}_{hk} \approx \bar{Y}_{hk}^* . \quad (60)$$

Equation (60) allows simplifying (32) as:

$$\dot{\bar{s}} - \bar{s} \circ \bar{\eta} \approx \bar{Y}^* \bar{\eta}^* , \quad (61)$$

and (39) and (41) as:

$$\dot{\bar{i}} \approx \bar{Y} \bar{\eta} . \quad (62)$$

One can further simplify the expressions above for high-voltage transmission systems, for which  $\bar{Y} \approx j\mathbf{B}$ :

$$\dot{\bar{s}} - \bar{s} \circ \bar{\eta} \approx -j\mathbf{B} \bar{\eta}^* , \quad (63)$$

and (39) and (41) as:

$$\dot{\bar{i}} \approx j\mathbf{B} \bar{\eta} . \quad (64)$$

Then, approximating the term  $\bar{s} \circ \bar{\eta} \approx \bar{Y}_{\text{diag}}^* \bar{\eta}$ , where  $\bar{Y}_{\text{diag}}$  is a matrix obtained using the diagonal elements of  $\bar{Y}$ , and splitting the real and imaginary part of  $\bar{\eta}$ , (63) leads to:

$$\dot{\mathbf{p}}' \approx \mathbf{B}' \boldsymbol{\omega} , \quad (65)$$

where  $B'_{hk} = -B_{hk}$  and  $B'_{hh} = \sum_{h \neq k}^n B_{hk}$  are the elements of  $\mathbf{B}'$ , and

$$\dot{\mathbf{q}}'' \approx \mathbf{B}'' \boldsymbol{\rho} , \quad (66)$$

where  $B''_{hk} = -B_{hk}$  and  $B''_{hh} = -2B_{hh}$  are the elements of  $\mathbf{B}''$ . Equation (65) is the expression deduced in [7] and that, with due simplifications, leads to the frequency divider formulas presented in [5].

Considering the resistive parts of the network branches, the following dual expressions hold:

$$\dot{\mathbf{p}}' \approx \mathbf{G}' \boldsymbol{\rho} , \quad \dot{\mathbf{q}}' \approx \mathbf{G}' \boldsymbol{\omega} , \quad (67)$$

where the elements of  $\mathbf{G}'$  and  $\mathbf{G}''$  are defined as  $G'_{hk} = G''_{hk} = -G_{hk}$ ,  $G'_{hh} = \sum_{h \neq k}^n G_{hk}$ , and  $G''_{hh} = -2G_{hh}$ . Interestingly, from (67), it descends that, in lossy networks, the reactive power can be utilized to regulate the frequency.

Combining together (65), (66) and (67) leads to the following approximated expressions:

$$\dot{\bar{s}}' \approx j\bar{Y}'^* \boldsymbol{\omega} , \quad \dot{\bar{s}}'' \approx \bar{Y}'' \boldsymbol{\rho} . \quad (68)$$

#### IV. EXAMPLES

The examples presented below apply the theory developed in the previous section and discuss applications to power system modeling, state estimation and control. In particular, three devices are discussed, namely, the synchronous machine; the voltage dependent load; and a converter-interfaced generator with frequency and voltage control capability. The objective is to illustrate the methodological approach discussed above and showcase some problems that the proposed definition of complex frequency and the expression (32) make possible to solve. In the following, all simulation results are obtained using the software tool Dome [15].

##### A. Ratio between $\boldsymbol{\omega}$ and $\boldsymbol{\rho}$

This first example illustrates the transient behavior of the two components of the complex frequency. Figure 1 shows the transient behavior of the components of the complex frequency at a generator and a load bus, bus 2 and bus 8, respectively, for the well-known WSCC 9-bus system [9]. The estimation of  $\omega_h$  and  $\rho_h$  at the buses of the grid is obtained through a numerical differentiation based on a synchronous-reference frame Phase-Locked Loop (PLL) model [16]. Simulation results show that  $|\omega_h| \gg |\rho_h|$ . This inequality holds for all networks and scenarios that we have tested for the preparation of this work.

It is important to note that the inequality  $|\omega_h| \gg |\rho_h|$  does not imply  $\dot{s}'_h \gg \dot{s}''_h$ . As a matter of fact, taking as an example constant impedance loads,  $\dot{s}'_h = 0$  and  $\dot{s}''_h = \dot{s}_h$ . The rationale behind this observation can be explained by rewriting (35) using (17) and an element-by-element notation:

$$\begin{aligned} \dot{s}'_h &= j \sum_{k=1}^n \bar{s}_{hk} (\omega_h - \omega_k) , \\ \dot{s}''_h &= \sum_{k=1}^n \bar{s}_{hk} (\rho_h + \rho_k) , \end{aligned} \quad (69)$$

which indicates that  $\dot{s}'_h$  is proportional to the *difference* of the elements of  $\boldsymbol{\omega}$ , whereas  $\dot{s}''_h$  is proportional to the *sum* of the elements of  $\boldsymbol{\rho}$ . Hence, even if the elements of  $\boldsymbol{\rho}$  are small relatively to those of  $\boldsymbol{\omega}$ , their effect on the system are not necessarily negligible.

##### B. Implementation of Equation (32)

The implementation of (32) in a software tool for the simulation of power systems can be useful to determine the “exact” frequency variations at network buses in a QSS model for transient stability analysis. This topic has been discussed and solved under various hypotheses in [4]–[6]. In particular, the Frequency Divider Formula (FDF) proposed in [5] is based on (65), which is an approximation of (32).

The determination of  $\bar{\eta}$  requires the solution of the set of complex differential equations (32). These can be rewritten as a set of  $2n$  real equations, with unknowns  $(\boldsymbol{\rho}, \boldsymbol{\omega})$ . The right-hand side of (32) is linear with respect to  $\bar{\eta}$ , so it remains to determine the dependency of the elements of  $\dot{\bar{s}} - \bar{s} \circ \bar{\eta}^*$  or, alternatively, of  $\bar{v} \circ \dot{\bar{i}}^*$  from (39), on  $\bar{\eta}$  and, eventually, on the time derivative of the state variables  $\dot{\mathbf{x}}$ .

We illustrate the procedure using a conventional 4th order model of the synchronous machine. The stator voltage of the machine with respect to its dq-axis reference frame is linked to the grid voltage  $v_h$  with the following equations [9]:

$$\bar{v}_s = v_{s,d} + j v_{s,q} = \bar{v}_h \angle \left( \frac{\pi}{2} - \delta_r \right) , \quad (70)$$

where  $\delta_r$  is the rotor angle of the machine. The time derivative of (70) gives (see the Appendix for the derivative of  $\bar{v}_h$ ):

$$\dot{\bar{v}}_s = \bar{v}_s (\bar{\eta}_h - j \omega_r) , \quad (71)$$

where  $\omega_r$  is the deviation in rad/s of the angular speed of the machine with respect to  $\omega_o$ . Then, the stator electrical and magnetic equations are:

$$\begin{aligned} X'_d i_{s,d} + R_a i_{s,q} &= -v_{s,q} + e'_{r,q} \\ R_a i_{s,d} - X'_q i_{s,q} &= -v_{s,d} + e'_{r,d} \end{aligned} \quad (72)$$

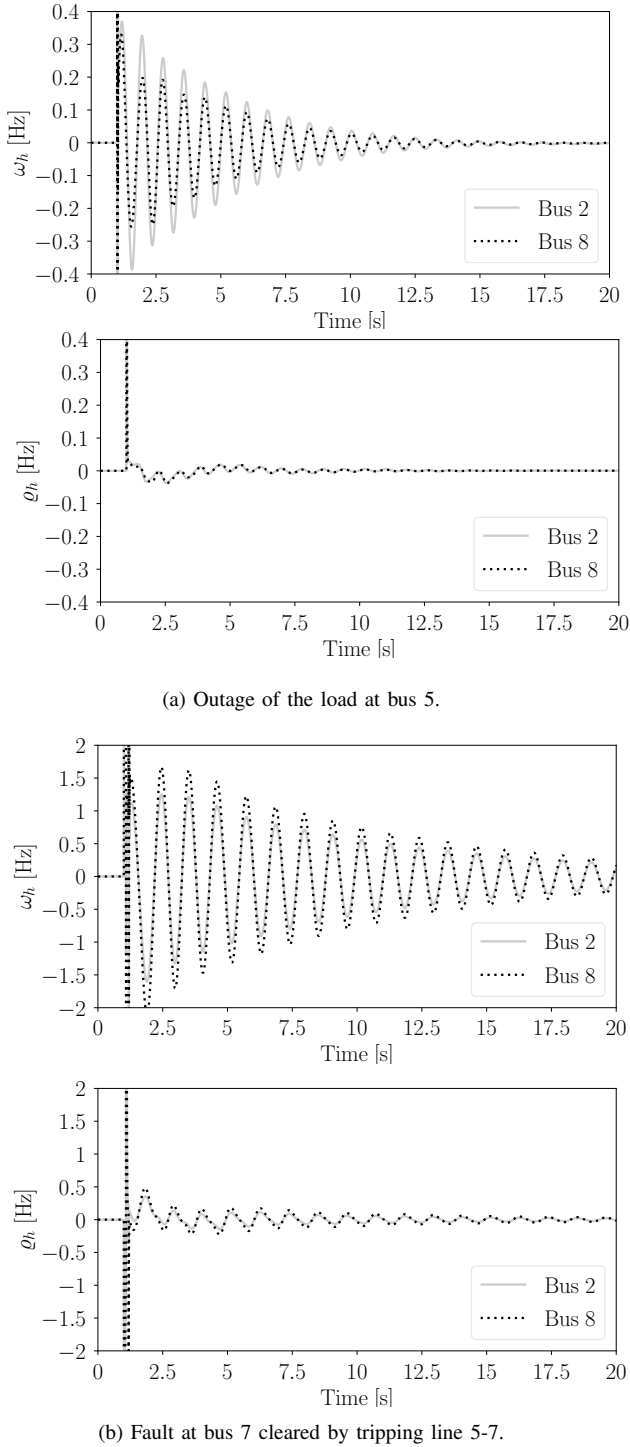


Fig. 1: Transient behavior of the components of the complex frequency for the WSCC 9-bus system.

where  $\bar{i}_s = i_{s,d} + j i_{s,q}$  is the stator current. From (72), one can thus obtain the expressions of  $i_{s,d}$  and  $i_{s,q}$  as a function of  $v_{s,d}$ ,  $v_{s,q}$  and the state variables  $e'_{r,d}$  and  $e'_{r,q}$ . In this case, these relationships are linear, so, the time derivatives of the components of the current give:

$$\begin{aligned} i_{s,d} &= \frac{\partial i_{s,d}}{\partial \omega_h} \omega_h + \frac{\partial i_{s,d}}{\partial \varrho_h} \varrho_h + \frac{\partial i_{s,d}}{\partial \omega_r} \omega_r + \frac{\partial i_{s,d}}{\partial e'_{r,d}} \dot{e}'_{r,d} + \frac{\partial i_{s,d}}{\partial e'_{r,q}} \dot{e}'_{r,q}, \\ i_{s,q} &= \frac{\partial i_{s,q}}{\partial \omega_h} \omega_h + \frac{\partial i_{s,q}}{\partial \varrho_h} \varrho_h + \frac{\partial i_{s,q}}{\partial \omega_r} \omega_r + \frac{\partial i_{s,q}}{\partial e'_{r,d}} \dot{e}'_{r,d} + \frac{\partial i_{s,q}}{\partial e'_{r,q}} \dot{e}'_{r,q}, \end{aligned} \quad (73)$$

where the time derivative of  $v_{s,d}$  and  $v_{s,q}$  have been substituted with the real and imaginary parts of the left-hand side of (71). Finally, from (39), one obtains:

$$\begin{aligned} \text{Re}\{\bar{v}_h \dot{i}_h^*\} &= \text{Re}\{\bar{v}_s \dot{i}_s^*\} = v_{s,d} \dot{i}_{s,d} + v_{s,q} \dot{i}_{s,q}, \\ \text{Im}\{\bar{v}_h \dot{i}_h^*\} &= \text{Im}\{\bar{v}_s \dot{i}_s^*\} = v_{s,q} \dot{i}_{s,d} - v_{s,d} \dot{i}_{s,q}. \end{aligned} \quad (74)$$

Finally, substituting (73) into (74), one obtains the expressions of the left-hand side of (39) at the buses of the synchronous machines.

The very same procedure can be applied to any device of the grid and, in the vast majority of the cases, the resulting expressions are linear with respect to  $(\varrho, \omega)$ . Hence, at each time step of a time domain simulation one needs to solve a problem of the type  $\mathbf{A}\chi = \mathbf{b}$ , where  $\chi = [\varrho^T, \omega^T]^T$ , and:

$$\mathbf{A} = \begin{bmatrix} [\mathbf{H} + \text{diag}(\mathbf{p}) - \mathbf{P}_\varrho] & [\mathbf{K} - \text{diag}(\mathbf{q}) - \mathbf{P}_\omega] \\ [\mathbf{K} + \text{diag}(\mathbf{q}) - \mathbf{Q}_\varrho] & -[\mathbf{H} - \text{diag}(\mathbf{p}) + \mathbf{Q}_\omega] \end{bmatrix} \quad (75)$$

and

$$\mathbf{b} = \begin{bmatrix} \mathbf{P}_x \dot{\mathbf{x}} \\ \mathbf{Q}_x \dot{\mathbf{x}} \end{bmatrix}, \quad (76)$$

where  $\mathbf{H} = \text{Re}\{\bar{\mathbf{S}}\}$  and  $\mathbf{K} = \text{Im}\{\bar{\mathbf{S}}\}$ ;  $\mathbf{P}_\varrho$ ,  $\mathbf{P}_\omega$ ,  $\mathbf{Q}_\varrho$  and  $\mathbf{Q}_\omega$  are the Jacobian  $n \times n$  matrices of  $\mathbf{p}$  and  $\mathbf{q}$  with respect to  $\varrho$  and  $\omega$ , respectively; and  $\mathbf{P}_x$  and  $\mathbf{Q}_x$  are the Jacobian  $n \times n_x$  matrices of  $\mathbf{p}$  and  $\mathbf{q}$  with respect to the state variables  $\mathbf{x}$ , respectively.

Figure 2 shows the imaginary part of the complex frequency as obtained for the WSCC 9-bus system using a 4th and a 2nd order model of the synchronous machines, as well as for a scenario where the machine at bus 3 is substituted for a Converter-Interfaced Generator (CIG). The model of the CIG is shown in Fig. 3. The results obtained using PLLs match well the “exact” results obtained with the proposed method (indicated with CF in the legends) except for the numerical spikes that follow the load disconnection and a small delay that is due to the control loop of the PLL. The proposed formula is also robust with respect to noise as shown in Fig. 2b. Figure 2 also shows the results obtained using the FDF proposed in [5]. The FDF matches closely the results of the proposed method when considering the simplified 2nd order model of the machines but introduces some errors if the machine model includes rotor flux dynamics or when considering the CIG.

### C. Voltage Dependent Load (VDL)

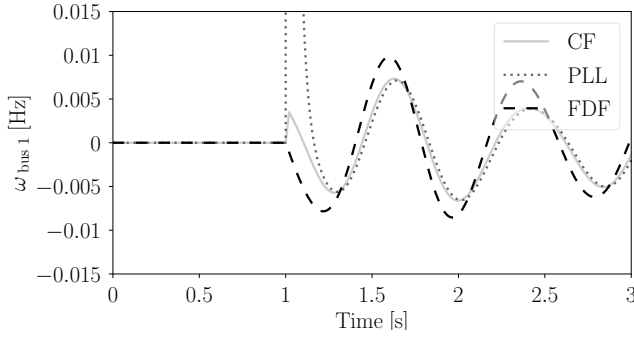
The power consumption of a VDL is:

$$\bar{s}_h = p_h + j q_h = -p_o v_h^{\gamma_p} - j q_o v_h^{\gamma_q}, \quad (77)$$

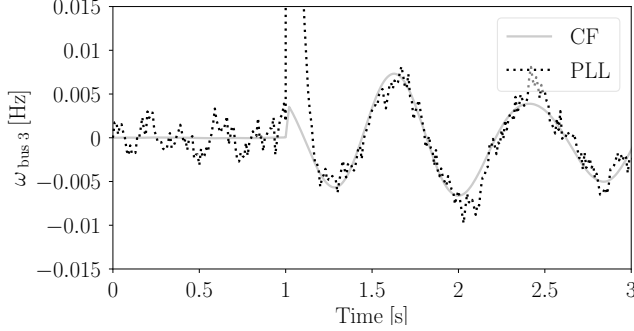
then:

$$\begin{aligned} \dot{\bar{s}}_h &= -p_o \gamma_p \dot{v}_h v_h^{\gamma_p-1} - j q_o \gamma_q \dot{v}_h v_h^{\gamma_q-1} \\ &= (\gamma_p p_h + j \gamma_q q_h) \varrho_h, \end{aligned} \quad (78)$$

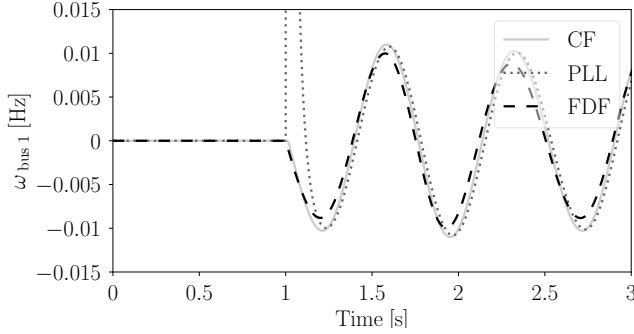
where it has been assumed that the exponents  $\gamma_p$  and  $\gamma_q$  are constant and that  $p_o$  and  $q_o$  vary “slowly” with respect to  $v_h$ . If  $\gamma_p = \gamma_q = \gamma$ , then  $\dot{\bar{s}}_h = \gamma \bar{s}_h \varrho_h$ , which generalizes the results obtained in Section III-C.2.



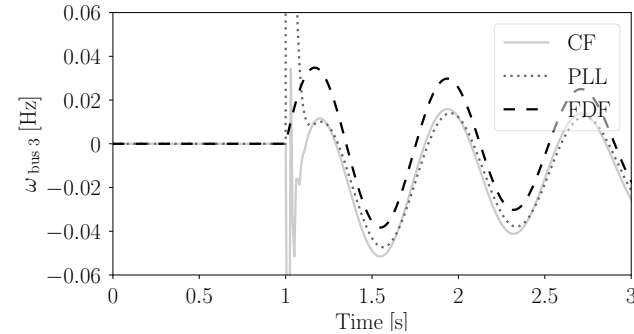
(a) 4th order machine models



(b) 4th order machine models &amp; noise



(c) 2nd order machine models



(d) CIG connected at bus 3

Fig. 2: Comparison of bus frequencies using PLL, FDF and the proposed approach based on the complex frequency. The plots refers to the WSCC 9-bus system following the disconnection at  $t = 1$  s of the load at bus 5.

As an application, we utilize (78) to estimate the parameters  $\gamma_p$  and  $\gamma_q$  of a VDL using a similar technique as the one proposed in [13]. From (32) and (78), one obtains:

$$(\gamma_p p_h + j \gamma_q q_h) \varrho_h = \sum_{k=1}^n [\bar{s}_{hk} (\bar{\eta}_h + \bar{\eta}_k^*)], \quad (79)$$

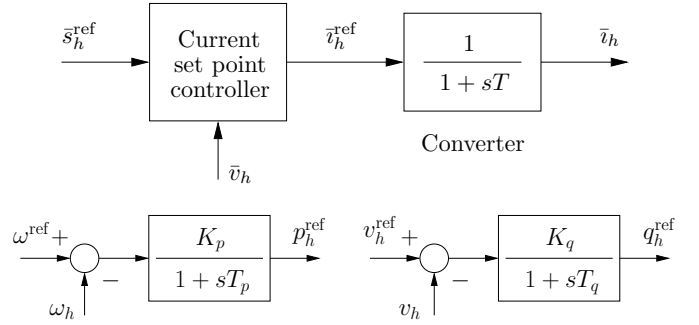


Fig. 3: Simplified scheme of a CIG and its controllers.

and, splitting real and imaginary parts:

$$\begin{aligned} \gamma_p &= (p_h \varrho_h)^{-1} \operatorname{Re} \left\{ \sum_{k=1}^n \bar{s}_{hk} (\bar{\eta}_h + \bar{\eta}_k^*) \right\}, \\ \gamma_q &= (q_h \varrho_h)^{-1} \operatorname{Im} \left\{ \sum_{k=1}^n \bar{s}_{hk} (\bar{\eta}_h + \bar{\eta}_k^*) \right\}, \end{aligned} \quad (80)$$

where the right-hand sides can be determined based on measurements. The fact that  $\varrho_h \rightarrow 0$  in steady-state can create numerical issues, which can be solved, as discussed in [13], using finite differences over a period of time  $\Delta t$ , namely  $\bar{\eta}_h \approx \Delta \bar{\zeta}_h / \Delta t$ ,  $\bar{\eta}_k^* \approx \Delta \bar{\zeta}_k^* / \Delta t$ , and  $\varrho_h \approx \Delta u_h / \Delta t$ , as follows:

$$\begin{aligned} \hat{\gamma}_p &\approx (p_h \Delta u_h)^{-1} \operatorname{Re} \left\{ \sum_{k=1}^n \bar{s}_{hk} (\Delta \bar{\zeta}_h + \Delta \bar{\zeta}_k^*) \right\}, \\ \hat{\gamma}_q &\approx (q_h \Delta u_h)^{-1} \operatorname{Im} \left\{ \sum_{k=1}^n \bar{s}_{hk} (\Delta \bar{\zeta}_h + \Delta \bar{\zeta}_k^*) \right\}. \end{aligned} \quad (81)$$

Equations (80) and (81) generalize the empirical formulas to estimate  $\gamma_p$  and  $\gamma_q$  proposed in [13]. The latter, in fact, can be obtained from (81) by approximating  $\bar{s}_{hk} \approx -j B_{hk}$ .

Figure 4 shows the results obtained for the WSCC 9-bus system where the bus connected at bus 8 is a VDL with  $\gamma_p = 2$  and  $\gamma_q = 1.5$ . The results show that (81) is, as expected, more precise than the approximated estimations based on the expression proposed in [13]. Equation (81) is, in fact, an exact expression and its accuracy depends exclusively on the accuracy of the measurements of  $\bar{\zeta}_h$  and  $\bar{\zeta}_k^*$ , which can be obtained, for example, with PMUs. If the  $R/X$  ratio of the transmission lines of the system is changed to resemble that of a distribution system, (81) appears also numerically more robust than its approximated counterparts (see Fig. 4b).

#### D. Converter-Interfaced Generation

This last example illustrates an application of the approximated expression (67). We focus in particular on the link between  $\omega$  and  $\dot{q}$  through the resistances of network branches. Using again the WSCC 9-bus system and substituting two synchronous machines with CIGs, we compare the dynamic response of the system following a load variation using the control scheme of Fig. 3 (Control 1), and the control scheme shown in Fig. 5 (Control 2). The latter regulates the frequency by both the active and reactive powers of the CIGs.

Figure 6 shows that Control 2 is more effective than Control 1 to reduce the variations of the frequency. This result indicates that the relationship between  $q$  and  $\omega$  is not weak and can be exploited to improve the frequency response of low-inertia systems. This result is predicted by (67) and hence by (32).



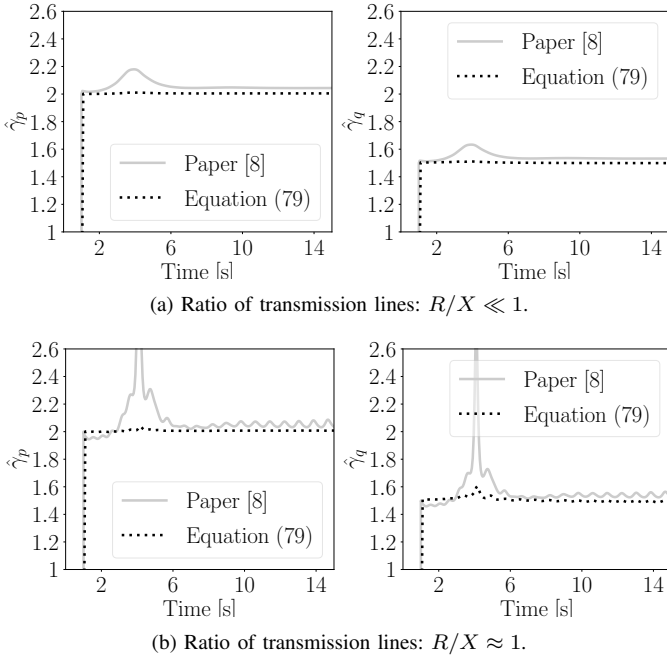


Fig. 4: Estimation of the exponents of the VDL connected at bus 8 following the disconnection of 15% of the load at bus 5 at  $t = 1$  s for the WSCC 9-bus system.

The simplified converter-interfaced generator model shown in Fig. 5, with differential equations:

$$\begin{aligned} T_p \dot{p}_h &= K_p (\omega^{\text{ref}} - \omega_h) - p_h, \\ T_q \dot{q}_h &= K_q (v^{\text{ref}} - v_h) - q_h. \end{aligned} \quad (82)$$

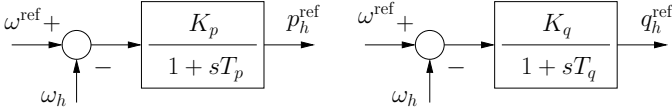


Fig. 5: Alternative frequency control through active and reactive powers for the CIG of Fig. 3.

## V. CONCLUSIONS

The paper introduces a new physical quantity, namely, the *complex frequency*. This quantity allows writing the differential of power flow equations in terms of complex powers and voltages at network buses. The most significant property of the newly defined complex frequency presented is its ability to give a much more robust and clean indication of frequency than what generally accepted in the literature, especially to describe the behavior of the frequency at buses close to a disturbance. For example, it is well known that many other methods result in meaningless spikes in frequency at the inception and clearing of faults and other sudden disturbances. The proposed definition provides a solution to this issue.

Noteworthy byproducts of the definition of the complex frequency are the expressions (32), (39) and (41). These equations express the formal link between the complex power and complex frequency variations and are a relevant contribution

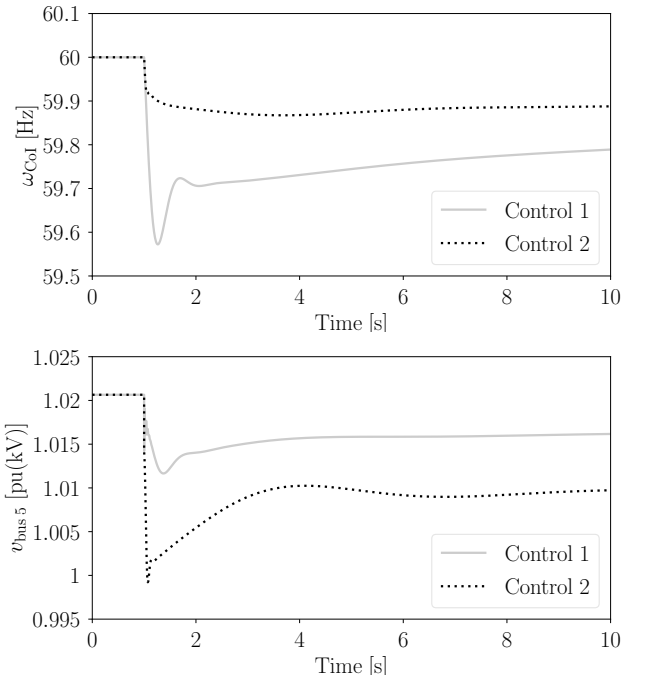


Fig. 6: Frequency of the CoI and voltage at bus 5 following the connection of  $p = 0.25$  pu at bus 5 at  $t = 1$  s for the WSCC 9-bus system with high penetration of CIG.

of the paper. The paper shows that the expressions above are a generalization of the FDF proposed in [5]. The several analytical and numerical examples discussed Sections III and IV show the several prospective applications of the proposed theoretical approach.

Future work will focus on further elaborating the expression (32) and exploiting its features for the control and state estimation of power systems. It also appears relevant to combine the proposed complex frequency approach to some of the techniques described in [3]. Particularly interesting, for example, is the “beyond-phasor” approach based on the Hilbert transform proposed in [17].

## APPENDIX

This appendix provides the proof of (37). With this aim, let us consider the  $h$ -th element of (37), namely  $\bar{v}_h = v_h \angle \theta_h = v_h (\cos \theta_h + j \sin \theta_h)$ . The time derivative of  $\bar{v}_h$  with respect to the dq-axis reference frame gives:

$$\begin{aligned} \dot{\bar{v}}_h &= \dot{v}_h \angle \theta_h + j v_h \omega_h \angle \theta_h \\ &= v_h (\dot{\varrho}_h \angle \theta_h + j \omega_h \angle \theta_h) \\ &= v_h \angle \theta_h (\dot{\varrho}_h + j \omega_h) \\ &= \bar{v}_h \bar{\eta}_h, \end{aligned}$$

where the following identities hold:

$$\begin{aligned} \frac{d}{dt} \angle \theta_h &= \omega_h (-\sin \theta_h + j \cos \theta_h) \\ &= j \omega_h (\cos \theta_h + j \sin \theta_h) \\ &= j \omega_h \angle \theta_h. \end{aligned}$$

## REFERENCES

- [1] “IEEE/IEC International Standard - Measuring relays and protection equipment - Part 118-1: Synchrophasor for power systems - Measurements,” pp. 1–78, 2018.
- [2] H. Kirkham, W. Dickerson, and A. Phadke, “Defining power system frequency,” in *IEEE PES General Meeting*, 2018, pp. 1–5.
- [3] M. Paolone, T. Gaunt, X. Guillaud, M. Liserre, S. Meliopoulos, A. Monti, T. Van Cutsem, V. Vittal, and C. Vournas, “Fundamentals of power systems modelling in the presence of converter-interfaced generation,” *Electric Power Systems Research*, vol. 189, p. 106811, 2020.
- [4] J. Nutaro and V. Protopopescu, “Calculating frequency at loads in simulations of electro-mechanical transients,” *IEEE Trans. on Smart Grid*, vol. 3, no. 1, pp. 233–240, 2012.
- [5] F. Milano and Á. Ortega, “Frequency divider,” *IEEE Trans. on Power Systems*, vol. 32, no. 2, pp. 1493–1501, 2017.
- [6] H. Golpîra and A. R. Messina, “A center-of-gravity-based approach to estimate slow power and frequency variations,” *IEEE Trans. on Power Systems*, vol. 33, no. 1, pp. 1026–1035, 2018.
- [7] F. Milano and Á. Ortega, “A method for evaluating frequency regulation in an electrical grid Part I: Theory,” *IEEE Trans. on Power Systems*, 2020, in press.
- [8] —, *Frequency Variations in Power Systems: Modeling, State Estimation, and Control*. Hoboken, NJ: Wiley, 2020.
- [9] P. W. Sauer and M. A. Pai, *Power System Dynamics and Stability*. Upper Saddle River, NJ: Prentice Hall, 1998.
- [10] F. Milano, *Power System Modelling and Scripting*. London, UK: Springer, 2010.
- [11] U. M. Ascher and L. R. Petzold, *Computer Methods for Ordinary Differential Equations and Differential-Algebraic Equations*, 1st ed. USA: Society for Industrial and Applied Mathematics, 1998.
- [12] H. Stephani, *Differential Equations: Their Solution Using Symmetries*, M. MacCallum, Ed. Cambridge University Press, 1990.
- [13] Á. Ortega and F. Milano, “Estimation of voltage dependent load models through power and frequency measurements,” *IEEE Trans. on Power Systems*, vol. 35, no. 4, pp. 3308–3311, 2020.
- [14] B. Stott and O. Alsac, “Fast decoupled load flow,” *IEEE Trans. on Power Systems*, vol. PAS-93, no. 3, pp. 859–869, 1974.
- [15] F. Milano, “A Python-based software tool for power system analysis,” in *IEEE PES General Meeting*, 2013, pp. 1–5.
- [16] Á. Ortega and F. Milano, “Comparison of different PLL implementations for frequency estimation and control,” in *ICHQP*, 2018, pp. 1–6.
- [17] A. Derviskadić, G. Frigo and M. Paolone, “Beyond phasors: Modeling of power system signals using the Hilbert transform,” in *IEEE Trans. on Power Systems*, vol. 35, no. 4, pp. 2971–2980, 2020.



**Federico Milano** (F'16) received from the University of Genoa, Italy, the M.E. and Ph.D. in Electrical Engineering in 1999 and 2003, respectively. From 2001 to 2002, he was with the Univ. of Waterloo, Canada. From 2003 to 2013, he was with the Univ. of Castilla-La Mancha, Spain. In 2013, he joined the Univ. College Dublin, Ireland, where he is currently Professor of Power Systems Control and Protections and Head of Electrical Engineering. His research interests include power systems modeling, control and stability analysis.